Nearest-Neighbor Parameters for G·U Mismatches: $^{5'GU3'}_{3'UG5'}$ Is Destabilizing in the Contexts $^{CGUG}_{GUGC}$, $^{UGUA}_{AUGU}$, and $^{AGUU}_{UUGA}$ but Stabilizing in $^{GGUC}_{CUGG}$†

Liyan He,‡ Ryszard Kierzek,§ John SantaLucia, Jr.,‡ Amy E. Walter,‡ and Douglas H. Turner*,‡

Department of Chemistry, University of Rochester, Rochester, New York 14627-0216, and Institute of Bioorganic Chemistry, Polish Academy of Sciences, 60-704 Poznan, Noskowskiego 12/14 Poland

Received July 8, 1991; Revised Manuscript Received August 29, 1991

ABSTRACT: Thermodynamic parameters derived from optical melting studies are reported for duplex formation by a series of oligoribonucleotides containing G·U mismatches. The results are used to determine nearest-neighbor parameters for helix propagation by G·U mismatches. Surprisingly, the $^{5'GU3'}_{3'UG5'}$ nearest-neighbor free energy increment is unfavorable in the contexts $^{CGUG}_{GUGC}$, $^{UGUA}_{AUGU}$, and $^{AGUU}_{UUGA}$ but favorable in the context $^{GGUC}_{CUGG}$. This is a non-nearest-neighbor effect. In contrast, the $^{5'UG3'}_{3'GU5'}$ free energy increment is favorable and independent of context. Circular dichroism and imino proton NMR spectra of several sequences do not reveal an obvious structural basis for this dichotomy. For example, all the G·U mismatches have two slowly exchanging imino protons. The imino resonances for the G·U mismatches in GGAGUUCC, GUCGUGAC, and CCUGUAGG, however, broaden at lower temperature than the imino resonances for the interior Watson–Crick base pairs. In contrast, the imino resonances for the G·U mismatches in GGAUGUCC remain sharp at high temperature. The improved parameters for G·U mismatches should improve predictions of RNA structure from sequence.

RNAs have important biological functions such as transcription, translation, and catalysis (Watson et al., 1987). Understanding the molecular basis of these functions requires knowledge of three-dimensional structures of RNAs. Because of the large size of most RNAs of interest and the difficulty in growing RNA crystals, it is hard to determine RNA structures directly with physical techniques. Thus, modeling based on phylogeny and other data has been used to provide insight into three-dimensional structures of RNA (Stern et al., 1988; Michel & Westhof, 1990; Kim & Cech, 1987).

Prediction of secondary structures by free energy minimization is a first step toward prediction of three-dimensional structures (Tinoco et al., 1971, 1973; Turner et al., 1988; Zuker, 1989; Jaeger et al., 1989). In this method, it is assumed that RNA secondary structures are determined largely by nearest-neighbor interactions that can be measured in model systems. Application of this method, however, requires a large data bank of parameters for the nearest-neighbor interactions (Tinoco et al., 1973; Freier et al., 1986a; Turner et al., 1988). Fortunately, advances in RNA synthesis (Kierzek et al., 1986; Milligan et al., 1987; Usman et al., 1987) make it possible to study molecules with many different structural motifs.

This work focuses on the thermodynamic parameters for G·U mismatches. Crick (1966) proposed a special stability for G·U mismatches. Since then, G·U mismatches have been observed in tRNA (Kim et al., 1974; Ladner et al., 1975; Sussman & Kim, 1976; Johnston & Redfield, 1981; Sprinzl et al., 1985) and in proposed secondary structures of all large RNA molecules (Fox & Woese, 1975; Kime & Moore, 1983; Noller, 1984; Erdmann et al., 1985; Woese et al., 1983; Steger et al., 1984; Cech et al., 1983; Stern et al., 1988). For example, there are about 15% as many G·U mismatches as Watson–Crick base pairs in the secondary structures of *Escherichia coli* 16S rRNA (Stern et al., 1988) and the group I self-splicing LSU intron from *Tetrahymena thermophila* (Burke et al., 1987; Michel et al., 1982; Davies et al., 1982). Knowledge of the thermodynamics and structures of G·U mismatches is therefore important for improving RNA structure prediction.

Despite the prevalence of G·U mismatches, there are only limited studies of their thermodynamics. The stability of terminal G·U pairs is close to that of corresponding A·U pairs (Uhlenbeck et al., 1971; Freier et al., 1986b; Sugimoto et al., 1987), consistent with the wobble hypothesis (Crick, 1966). Results for internal G·U mismatches, however, are complicated. Early work suggested addition of an internal G·U mismatch neither increases nor decreases the stability of a complementary helix (Uhlenbeck et al., 1971; Romaniuk et al., 1979a,b). Studies of other sequences, however, showed the effect of an internal G·U pair on stability depends on the flanking Watson–Crick pairs (Alkema et al., 1982; Sugimoto et al., 1986). Six of the 11 possible nearest-neighbor parameters were provided by Sugimoto et al. (1986), but the parameters were derived from a limited data set. In this work, parameters for all 11 nearest-neighbor interactions involving G·U mismatches are derived from new and existing thermodynamic data (Sugimoto et al., 1986; Freier et al., 1986b). The new sequences include duplexes containing both isolated and adjacent G·U mismatches. It is found that ΔG°_{37} for propagation of a helix by a G·U mismatch adjacent to a complementary base pair is usually similar to that for propagation by the corresponding AU base pair. The ΔG°_{37} values for propagation of a helix by a G·U mismatch adjacent to another G·U mismatch, however, are complex. The thermodynamics of $^{5'UG3'}_{3'GU5'}$ sequences are different from those of $^{5'GU3'}_{3'UG5'}$

† Supported by NIH Grant GM22939.
* Author to whom correspondence should be addressed.
‡ University of Rochester.
§ Polish Academy of Sciences.

0006-2960/91/0430-11124$02.50/0

sequences. There are non-nearest-neighbor interactions in $^{5'GU3'}_{3'UG5'}$ sequences. The parameters derived in this work provide more reliable prediction of stabilities of duplexes with G·U mismatches and should improve RNA secondary structure predictions. Some structural aspects of G·U mismatches are also explored with NMR and CD spectroscopies.

Materials and Methods

Oligonucleotide Synthesis and Purification. Oligonucleotides not reported elsewhere were synthesized on solid support by using a phosphoramidite approach with the 2'-hydroxyl protected by tetrahydropyranyl (Markiewicz et al., 1984; Kierzek et al., 1986). Oligonucleotides were removed from support and partially deblocked by treatment with 30% aqueous ammonia solution. The crude mixture was purified by either of the following methods: (a) HPLC on a PRP-1 semipreparative column (Hamilton) with a gradient of 0 to about 50% acetonitrile buffered with 10 mM ammonium acetate, pH 7. After removal of the acid-labile protecting groups, the oligonucleotide was desalted and further purified with a Sep-pak C-18 cartridge (Waters). (b) Acid-labile protecting groups were removed from the crude mixture, which was then purified on a Si500F TLC plate (J. T. Baker) (Chou et al., 1989). After development in ammonia/1-propanol/water (35:55:10 by volume) for 6 h, the least mobile band was cut out and eluted three times with 1 mL of double-distilled water. The RNA oligomer was then concentrated by evaporation, desalted, and further purified on a G-10 column (Sigma) eluted with water. Purities of the oligomers were checked by HPLC on a C8 analytical column (Hamilton) and were over 95% pure.

Melting Curves and Thermodynamic Parameters. Thermodynamic parameters were measured in 1 M NaCl, 10 mM sodium cacodylate, and 0.5 mM disodium ethylenediaminetetraacetate (Na_2EDTA), pH 7. Oligonucleotide concentrations (C_T) are strand concentrations and were calculated from the high-temperature absorbance at 280 nm. Single-strand extinction coefficients were calculated as described previously (Freier et al., 1983). Absorbance versus temperature melting curves were measured at 280 nm with a heating rate of 1 °C/min as described by Petersheim and Turner (1983). Thermodynamic parameters of helix formation were obtained from absorbance vs temperature profiles by two methods: (1) enthalpies and entropies from fits of individual melting curves to a two-state model with sloping base lines were averaged (Petersheim & Turner, 1983), and (2) plots of reciprocal melting temperature (T_M^{-1}) vs log C_T gave enthalpies and entropies (Borer et al., 1974):

$$T_M^{-1} = (2.3R/\Delta H^\circ) \log C_T + \Delta S^\circ/\Delta H^\circ \qquad (1)$$

Nearest-Neighbor Parameters for G·U Mismatches. Enthalpy and free energy changes for nearest-neighbor interactions involving G·U mismatches were derived by multiple linear regression (Bevington, 1969) to observed enthalpy and free energy changes upon the nearest-neighbor model (Borer et al., 1974; Freier et al., 1986a). The observed changes were defined as the sum of enthalpy or free energy increments for all the nearest-neighbor interactions involving G·U mismatches. These were calculated from parameters of helix formation for helixes with and without G·U mismatches, along with parameters for Watson–Crick interactions that are interrupted. For example, the observed free energy changes, ΔG°_{obs}, for nearest-neighbor interactions involving G·U mismatches in GGCGUGCC, GGCGUC, and GGCGCU, respectively, were calculated as follows:

$$\text{GGCGUGCC: } \Delta G^\circ_{obs}(^{CGUG}_{GUGC}) = 2\Delta G^\circ(^{5'CG3'}_{3'GU5'}) + \Delta G^\circ(^{5'GU3'}_{3'UG5'}) = \Delta G^\circ(\text{GGCGUGCC}) - \Delta G^\circ(\text{GGCGCC}) + \Delta G^\circ(^{5'CG3'}_{3'GC5'})$$

$$\text{GGCGUC: } \Delta G^\circ_{obs}(2^{GGG}_{CUG}) = 2\Delta G^\circ(^{5'GG3'}_{3'CU5'}) + 2\Delta G^\circ(^{5'GC3'}_{3'UG5'}) = \Delta G^\circ(\text{GGCGUC}) - \Delta G^\circ(^{5'CG3'}_{3'GC5'}) - \Delta G^\circ_i - \Delta G^\circ_{sym}$$

$$\text{GGCGCU: } \Delta G^\circ_{obs}(2^{GG}_{UC}) = 2\Delta G^\circ(^{5'GG3'}_{3'UC5'}) = \Delta G^\circ(\text{GGCGCU}) - \Delta G^\circ(\text{GCGC})$$

Here ΔG°_i is the free energy change for duplex initiation, 3.4 kcal/mol, and ΔG°_{sym} is the symmetry correction factor, 0.4 kcal/mol (Freier et al., 1986a). Here and henceforth, underlined nucleotides are in G·U mismatches. Parameters derived from T_M^{-1} vs log C_T plots were used to be consistent with previous work (Freier et al., 1986a). Parameters for oligomers that did not melt in two-state transitions were considered unreliable and were not included in the regression analysis. Experimental data were weighted (Wentworth, 1965) by the standard deviation calculated as described previously (SantaLucia et al., 1991). For Watson–Crick nearest-neighbor parameters, the error from regression analysis was used (Freier et al., 1986a) and the weights for observed enthalpy or free energy changes of G·U mismatches were calculated as illustrated for GGCGUGCC:

$$\sigma^2\Delta G^\circ_{obs}(^{CGUG}_{GUGC}) = \sigma^2\Delta G^\circ(\text{GGCGUGCC}) + \sigma^2\Delta G^\circ(\text{GGCGCC}) + \sigma^2\Delta G^\circ(^{5'CG3'}_{3'GC5'})$$

Circular Dichroism (CD) Spectroscopy. CD spectra were measured on a Jasco J40S spectropolarimeter. The same buffer was used as in the melting experiments. The measured CD was converted to $\Delta\epsilon$ as described by Cantor and Schimmel (1980).

NMR Spectroscopy. Imino proton NMR spectra were recorded on a Varian VXR-500S spectrometer. Oligomers were dissolved in a 10% D_2O and 90% H_2O solution of 0.08 M NaCl, 10 mM sodium phosphate, and 0.5 mM Na_2EDTA. One-dimensional imino proton spectra were acquired into 16000 complex points with a 1:3̄:3:1̄ solvent-suppression pulse sequence (Hore, 1983). A spectral width of 12 kHz was employed with the carrier frequency set at the water resonance and the delays set to maximize signal to noise at ~12 ppm. For NOE difference spectra, experiments with irradiation on- and off-resonance were collected in blocks of 16 scans and interleaved to correct for long-term instrumental drift. The 1:3̄:3:1̄ pulse sequence was used as the read pulse. A presaturation period of 1 s was used and the saturation power level was set to suppress 80% of each resonance. Sodium 3-(trimethylsilyl)tetradeuteriopropionate (TSP) was used as the internal standard in all the NMR experiments.

Results

Thermodynamic Parameters. Figure 1 shows typical plots of T_M^{-1} vs log C_T (see eq 1). Thermodynamic parameters of helix formation derived from these plots and from fitting the shape of each melting curve to the two-state model are listed in Table I. Also listed in Table I are thermodynamic parameters for reference oligomers.

The model used to obtain thermodynamic parameters from melting data assumes the helix to coil transition is two state. Typically, agreement within 15% for ΔH°s from curve fitting and from log C_T plots is considered a reasonable indication of a two-state transition (Freier et al., 1986a; Turner et al., 1988; Albergo et al., 1981; Petersheim & Turner, 1983; Hickey & Turner, 1985; Breslauer et al., 1975). Most of the oligomers

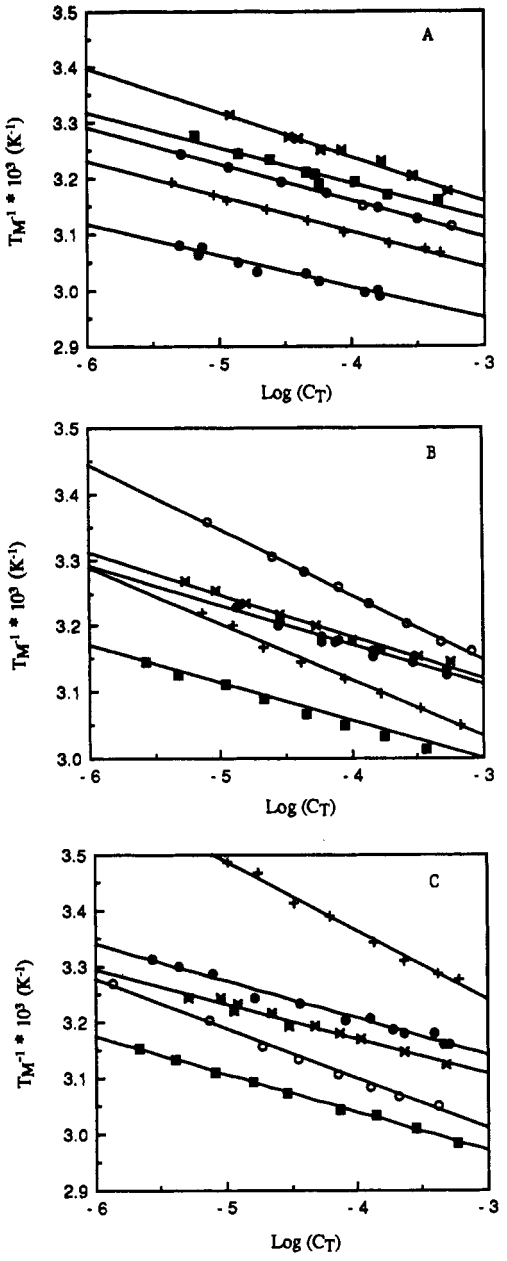

FIGURE 1: Plots of T_M^{-1} vs log (C_T): (A) CGGGUCCG (●), CUGGUCAG (○), AUGGUCAU (*), GGAGUUCC (■), and GGAUGUCC (+); (B) CGGAUUCG (*), GGCGUGCC (■), CCUGUAGG (●), GGAUCC (+), and CGUACG (○); (C) AGGCUU (+), GUCGUGAC (●), CGUUGACG (*), CCUAGG (○), and GCUGGCG (■).

listed in Table I meet this criterion. Exceptions are GUAGCUGC, UGGCUA, and GGUGUACC.

Thermodynamic Effects of Adding G·U Mismatches to Helixes. The change in thermodynamic parameters for duplex formation after addition of G·U mismatches is defined as $\Delta\Delta G^\circ = \Delta G^\circ$(duplex with G·U mismatches) − ΔG°(duplex without G·U mismatches). For example, the change in free energy at 37 °C, $\Delta\Delta G^\circ_{37}$, for insertion of the adjacent G·U mismatches in GGCGUGCC is $\Delta\Delta G^\circ_{37} = \Delta G^\circ_{37}$(GGCGUGCC) − ΔG°_{37}(GGCGCC). These changes are listed in Table II. Most of the free energy changes are negative so that addition of G·U mismatches usually increases the stability of a helix. Strikingly, however, duplexes with the motifs $\overset{CGUG}{GUGC}$, $\overset{UGUA}{AUGU}$, and $\overset{AGUU}{UUGA}$ are about 1 kcal/mol less stable than the duplexes without the G·U mismatches. This contrasts with insertion of the $\overset{5'UG3'}{3'GU5'}$ motif, which stabilizes duplexes by 1 to 2 kcal/mol.

Nearest-Neighbor Parameters. As described under Materials and Methods, the results in Table I can be used to calculate ΔG°_{obs} for the sum of nearest-neighbor interactions involving G·Us in each duplex. These values are listed in Table II. When the results for all 26 molecules are fitted to the nearest-neighbor model, the fit is poor. Exclusion of sequences with terminal G·Us does not improve the fit. Exclusion either of sequences with GGUC or with CGUG, UGUA, and AGUU, however, does give a good fit. The two sets of parameters derived are listed in Table III. Parameters for nearest-neighbor interactions of G·U base pairs with adjacent Watson–Crick base pairs, $\overset{XG}{YU}$ or $\overset{XU}{YG}$ ($\overset{X}{Y}$ is any Watson–Crick base pair), are essentially the same in both sets of parameters. (They are also essentially the same when all sequences are included in the fit.) The only parameter that is different in the two sets is that of $\overset{5'GU3'}{3'UG5'}$. When molecules with CGUG, UGUA, and AGUU are included with GGUC sequences excluded, ΔG° for the $\overset{5'GU3'}{3'UG5'}$ nearest neighbor is an unfavorable +1.5 kcal/mol. When molecules with GGUC are included with CGUG, UGUA, and AGUU excluded, ΔG° for the $\overset{5'GU3'}{3'UG5'}$ nearest neighbor is a favorable −1.0 kcal/mol. Evidently, the stability of the $\overset{5'GU3'}{3'UG5'}$ nearest neighbor is dependent on the flanking base pairs. This is a non-nearest-neighbor effect.

Circular Dichroism (CD) Spectra. CD spectra of GGAUGUCC, GGAGUUCC, CCUGUAGG, GUCGUGAC, AUGGUCAU, and a fully Watson–Crick-paired helix GGAUCC in 1 M NaCl at 0 °C are shown in the supplementary material (see paragraph at end of paper regarding supplementary material). All spectra have broad positive bands in the region of 240–290 nm. The only exception is AUGGUCAU, which has a negative band at 290 nm. The spectra of molecules with G·U mismatches are not dramatically different from that of the completely complementary duplex GGAUCC.

Imino Proton NMR Spectra. One-dimensional imino proton spectra of GGAGUUCC, GGAUGUCC, CCUGUAGG, and GUCGUGAC in H_2O are shown in Figure 2. Since all four duplexes are self-complementary octamers, there are only four different base pairs in each: a terminal G·C pair, an internal G·C pair, an internal A·U pair, and a G·U mismatch. There is one imino proton from each Watson–Crick base pair and two from each G·U mismatch. Thus, five slowly exchanging imino protons are expected for each duplex. All five imino proton resonances are clearly seen between 11.0 and 15.0 ppm for GUCGUGAC and CCUGUAGG at 0.5 °C. The terminal G·C imino protons of GGAGUUCC and GGAUGUCC are broad at 0.5 °C and overlap the resonances at ca. 12.5 ppm (spectra not shown). Thus, in Figure 2, spectra for GGAGUUCC and GGAUGUCC at 15 and 30 °C are shown, respectively. At these temperatures, all five resonances are resolved. Since imino protons from terminal base pairs exchange with solvent faster than those of internal base pairs, the imino protons of the terminal G·C pairs can be distinguished by their broad line widths. Imino protons from internal base pairs are well separated for all the molecules and their assignments by sequential NOE are therefore straightforward. This is illustrated in Figure 3 for GGAUGUCC. The AU imino proton at 14.4 ppm is identified by its strong NOE to the adenine H2 resonance at 7.9 ppm. The imino protons were then irradiated consecutively to assign the other base pairs. Some spin diffusion was observed from G2 (12.5 ppm) to the imino resonances at 11.8 and 11.2 ppm originating from the G·U mismatches and vice versa. Nevertheless, the

Table I: Thermodynamic Parameters of Helix Formation[a]

oligomers	T_M^{-1} vs log C_T plots: $-\Delta H°$ (kcal/mol)	$-\Delta S°$ (eu)	$-\Delta G°_{37}$ (kcal/mol)	T_M[b] (°C)	average of curve fits: $-\Delta H°$ (kcal/mol)	$-\Delta S°$ (eu)	$-\Delta G°_{37}$ (kcal/mol)	T_M[b] (°C)
Two-State Transitions[c]								
internal adjacent G·U								
GCUGGCG	67.7	187.1	9.58	56.0	72.1	201.0	9.80	55.8
AUGGUCAU	57.4	167.6	5.42	35.6	58.2	170.2	5.45	35.8
CCUGUAGG	71.1	207.3	6.81	42.0	66.1	191.1	6.81	42.4
CGGGUCCG	81.4	226.4	11.2	59.7	74.2	204.3	10.8	60.1
CGUUGACG	73.5	214.6	6.93	42.4	68.4	198.0	6.93	42.8
CUGGUCAG	70.5	204.4	7.10	43.4	64.1	184.0	7.02	43.7
GGAGUUCC	73.1	214.9	6.43	40.2	68.4	199.6	6.44	40.5
GGAUGUCC	73.0	208.4	8.39	49.0	78.0	223.4	8.59	49.0
GGCGUGCC	73.4	206.9	9.72	55.0	74.2	208.0	9.75	55.0
GUCGUGAC	69.1	203.3	6.05	38.7	64.7	188.9	6.08	39.0
GAGUUGAG	73.9	211.8	8.22	44.2	76.8	220.9	8.30	44.3
CUCGGCUC								
internal isolated G·U								
AGGCUU	37.1	106.6	4.07	24.2	34.6	97.9	4.24	24.7
AGUCGAUU	53.3	152.6	6.00	38.9	58.2	168.3	6.03	38.9
CGGAUUCG	72.6	213.0	6.56	40.8	70.3	205.4	6.59	41.1
reference helixes								
CCUAGG	54.1	149.1	7.80	49.7	59.7	166.5	8.07	50.0
CGUACG	46.6	133.1	5.35	34.8	35.9	98.2	5.50	34.0
GGAUCC	53.7	149.1	7.44	47.6	56.4	157.4	7.58	47.8
Non-Two-State Transitions[c]								
UGGCUA	49.7	143.0	5.36	35.0	36.1	98.5	5.54	35.8
GGUGUACC	65.8	193.1	5.94	38.3	49.6	140.6	5.99	39.0
GUAGCUGC	73.1	214.4	6.57	40.9	50.7	142.8	6.41	41.6

[a] Solutions are 1 M NaCl, 10 mM sodium cacodylate, and 0.5 mM Na_2EDTA, pH 7. Although errors in $\Delta G°$, $\Delta H°$, and $\Delta S°$ are roughly ±2%, ±10%, and ±10%, respectively, additional significant figures are given to allow accurate calculation of T_M and other parameters. Individual errors calculated as described by SantaLucia et al. (1991a,b) are given in the supplementary material for all sequences used to derive the nearest-neighbor parameters in Table III. [b] Calculated for 10^{-4} M strand concentration. [c] A transition is two state if the enthalpy change obtained from fitting the shapes of melting curves agrees within 15% with that obtained from plots of T_M^{-1} vs log C_T.

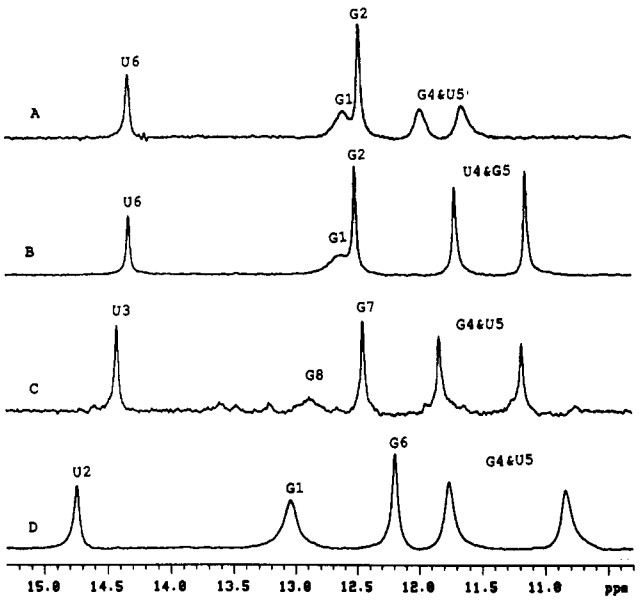

FIGURE 2: Imino proton NMR spectra (500 MHz) and NOE sequential assignments for (A) GGAGUUCC at 15 °C, pH 6.0; (B) GGAUGUCC at 30 °C, pH 5.5; (C) CCUGUAGG at 0.5 °C, pH 6.0; and (D) GUCGUGAC at 0.5 °C, pH 6.0. All samples are in a 10% D_2O and 90% H_2O solution of 0.08 M NaCl, 10 mM sodium phosphate, and 0.5 mM Na_2EDTA and the chemical shifts are referenced to TSP (sodium 3-(trimethylsilyl)tetradeuteriopropionate). Line broadening (4 Hz) is applied before Fourier transformation.

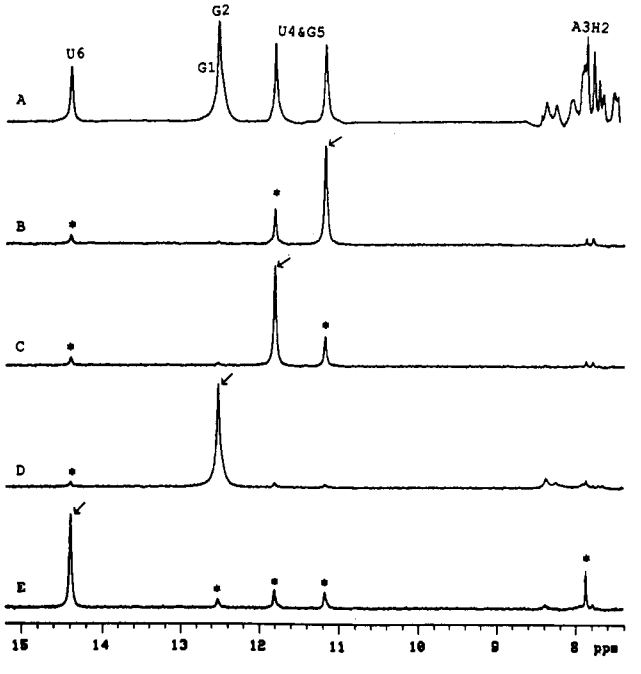

FIGURE 3: Imino proton difference NOE spectra of GGAUGUCC at 5 °C. Other conditions are the same as in Figure 2. (A) Control spectrum (no on-resonance irradiation within the spectrum); (B–E) difference spectra between a control spectrum and spectra obtained with 1-s saturation at 11.2, 11.8, 12.5, and 14.4 ppm, respectively. Saturation power levels were adjusted to result in about 80% saturation of the desired resonance. The saturated resonances are indicated by arrows while the observed NOEs are designated by asterisks. Small peaks between 11 and 13 ppm which are not designated by asterisks are from spin diffusion. Assignments are shown above spectrum A.

assignments are clear. Assignments of the imino protons of the G·U mismatches are confirmed by strong NOEs between resonances at 11.8 and 11.2 ppm. The strengths of the NOEs

Table II: Thermodynamic Increments and Observed Thermodynamic Parameter Changes for G·U Mismatches[a]

oligomers	increments for adding G·U[b]			observed parameter changes of G·U[c]	
	$\Delta\Delta G^\circ_{37}$ (kcal/mol)	$\Delta\Delta H^\circ$ (kcal/mol)	$\Delta\Delta S^\circ$ (eu)	$\Delta G^\circ_{37,obs}$ (kcal/mol)	ΔH°_{obs} (kcal/mol)
internal adjacent G·U					
GCUGGCG	−1.9 ± 0.1	−20.7 ± 2	−60.6 ± 5	−4.0 ± 0.1	−28.7 ± 2
GCUGGC[d]	−1.9 ± 0.03	−28.6 ± 2	−86.3 ± 6	−3.9 ± 0.1	−36.6 ± 2
CGUUGACG	−1.6 ± 0.1	−26.9 ± 4	−81.5 ± 12	−2.7 ± 0.1	−35.0 ± 4
AUGUGCAU[d]	−1.4 ± 0.05	−15.4 ± 2	−45.1 ± 7	−4.8 ± 0.1	−29.6 ± 2
GGAUGUCC	−1.0 ± 0.1	−19.3 ± 2	−59.3 ± 7	−1.9 ± 0.1	−25.0 ± 3
CGGGUCCG	−1.3 ± 0.3	−27.3 ± 5	−83.9 ± 16	−4.7 ± 0.3	−41.5 ± 5
AUGGUCAU	−0.7 ± 0.05	−15.7 ± 3	−48.3 ± 9	−4.1 ± 0.1	−29.9 ± 3
CUGGUCAG	−0.04 ± 0.04	−15.7 ± 2	−50.5 ± 6	−3.4 ± 0.1	−29.9 ± 2
CCUGUAGG	+1.0 ± 0.1	−17.0 ± 2	−58.3 ± 6	−0.1 ± 0.1	−25.1 ± 2
GGAGUUCC	+1.0 ± 0.1	−19.4 ± 7	−65.9 ± 21	+0.1 ± 0.1	−25.1 ± 7
GUCGUGAC	+1.0 ± 0.1	−15.5 ± 3	−53.3 ± 11	−1.0 ± 0.1	−23.5 ± 4
GGCGUGCC	+1.6 ± 0.1	−6.1 ± 1	−24.8 ± 4	−0.4 ± 0.1	−14.1 ± 2
GAGUUGAG	−0.8 ± 0.1	−19.9 ± 2	−61.9 ± 7	−3.7 ± 0.1	−32.1 ± 2
CUCGGCUC					
internal isolated G·U					
CGGCUG[d]	−1.9 ± 0.1	−12.9 ± 2	−35.5 ± 5	−5.9 ± 0.1	−2.09 ± 1
AGUCGAUU	−1.4 ± 0.1	−7.3 ± 2	−19.1 ± 6	−3.2 ± 0.1	−18.7 ± 2
AUGCGUp[d]	−1.3 ± 0.1	+4.9 ± 1	+19.9 ± 4	−4.6 ± 0.1	−10.3 ± 1
AUGCGCGUp[d]	−1.3 ± 0.1	−4.8 ± 2	−11.3 ± 5	−4.6 ± 0.1	−24.4 ± 2
AGGCUU[d]	−1.1 ± 0.1	−7.7 ± 2	−21.5 ± 6	−4.5 ± 0.1	−22.9 ± 2
CGGAUUCG	−0.8 ± 0.1	−24.3 ± 6	−75.7 ± 11	−5.4 ± 0.1	−50.8 ± 10
AUGCGUAUp[d]	−0.7 ± 0.1	−0.8 ± 2	−0.4 ± 7	−5.2 ± 0.1	−27.3 ± 2
GGCGUC	−0.06 ± 0.06	−7.6 ± 2	−24.4 ± 6	−6.1 ± 0.1	−30.1 ± 2
terminal isolated G·U					
GCCGGUp[e]	−4.7 ± 0.1	−24.0 ± 2	−62.4 ± 5	−4.7 ± 0.1	−24.0 ± 2
GGCGCU[e]	−3.8 ± 0.06	−25.9 ± 1	−71.6 ± 4	−3.8 ± 0.06	−25.9 ± 1
UGGCCGp[e]	−3.2 ± 0.1	−17.2 ± 2	−44.9 ± 5	−3.2 ± 0.1	−17.2 ± 2
UCCGGGp[e]	−2.8 ± 0.04	−13.5 ± 1	−34.4 ± 3	−2.8 ± 0.04	−13.5 ± 1
GAUGCAUUp[f]	−2.1 ± 0.05	−21.2 ± 3	−62.0 ± 8	−2.1 ± 0.05	−21.2 ± 3
UAUGCAUGp[f]	−1.8 ± 0.05	−20.6 ± 3	−61.0 ± 9	−1.8 ± 0.05	−20.6 ± 3

[a] Calculated from T_M^{-1} vs log C_T parameters. [b] Increments are defined as in the following example: for GUCGUGAC, $\Delta\Delta G^\circ$(GUCGUGAC) − ΔG°(GUCGAC). [c] Observed thermodynamic parameter changes of G·U mismatches are defined as the sum of thermodynamic parameters for nearest neighbors containing G·U. For example, ΔG°_{37}(obs) of GUCGUGAC is ΔG°_{37}(obs) = $\Delta G^\circ_{37}(^{CGUG}_{GUGC})$ = $2\Delta G^\circ_{37}(^{5'CG3'}_{3'GU5'})$ + $\Delta G^\circ_{37}(^{5'GU3'}_{3'UG5'})$ = ΔG°_{37}(GUCGUGAC) − ΔG°_{37}(GUCGAC) + $\Delta G^\circ_{37}(^{5'CG3'}_{3'GC5'})$. [d] Sugimoto et al. (1986). [e] Freier et al. (1986b). [f] Sugimoto et al. (1987).

Table III: Nearest-Neighbor Parameters for G·U Mismatches[a] and Comparison to Watson–Crick Base Pairs[b]

nearest neighbors	set I[c]			set II[d]			Watson–Crick base pairs[b]		
	ΔG°_{37}[e] (kcal/mol)	ΔH°[e] (kcal/mol)	ΔS°[e] (eu)	ΔG°_{37}[e] (kcal/mol)	ΔH°[e] (kcal/mol)	ΔS°[e] (eu)	ΔG°_{37} (kcal/mol)	ΔH° (kcal/mol)	ΔS° (eu)
$^{5'GC3'}_{3'UG5'}$	−2.1	−9.5	−23.9	−2.1	−9.5	−23.9	−2.1	−10.2	−26.2
$^{5'GG3'}_{3'UC5'}$	−1.9	−11.2	−30.1	−1.9	−11.2	−30.2	−1.7	−7.6	−19.2
$^{5'GG3'}_{3'CU5'}$	−1.4	−6.3	−15.8	−1.4	−6.3	−15.8	−2.3	−13.3	−35.5
$^{5'GA3'}_{3'UU5'}$	−1.1	−13.6	−40.2	−1.1	−13.6	−40.2	−0.9	−6.6	−18.4
$^{5'GU3'}_{3'UA5'}$	−1.0	−4.0	−9.7	−1.0	−4.1	−9.8	−0.9	−5.7	−15.5
$^{5'CG3'}_{3'GU5'}$	−1.2	−3.1	−6.2	−1.2	−3.1	−6.1	−1.8	−10.5	−27.8
$^{5'UG3'}_{3'AU5'}$	−0.8	−8.5	−24.9	−0.8	−8.6	−25.1	−1.1	−8.1	−22.6
$^{5'AG3'}_{3'UU5'}$	−0.5	−2.8	−7.2	−0.5	−2.6	−6.9	−0.9	−6.6	−18.4
$^{5'UG3'}_{3'GU5'}$	−0.2	−11.1	−34.9	−0.2	−11.0	−34.8	−1.1	−8.1	−22.6
$^{5'GU3'}_{3'UG5'}$	+1.5	−9.3	−35.1	−1.0	−18.3	−55.9	−0.9	−5.7	−15.5
$^{5'GG3'}_{3'UU5'}$	−0.4	−20.0	−63.1	−0.4	−20.0	−63.1	−0.9	−6.6	−18.4

[a] Parameters were derived by fitting thermodynamic parameters determined from T_M^{-1} vs log C_T plots for the molecules listed in Table II. [b] Parameters for the corresponding nearest neighbors in which G in each G·U mismatch is replaced by an A (Freier et al., 1986a). For example, $^{5'GC3'}_{3'UG5'}$ corresponds to $^{5'AC3'}_{3'UG5'}$. [c] Molecules with GGUC are not included in the fitting. [d] Molecules with CGUG, AGUU, and UGUA are not included in the fitting. [e] ΔG°_{37} and ΔH° were derived from fitting. The standard deviations between the measured values of ΔG°_{obs} and ΔH°_{obs} in Table II and the values calculated from the fitted parameters are 0.4 and 6 kcal/mol, respectively. ΔS° was calculated as follows: $\Delta S^\circ = (\Delta H^\circ - \Delta G^\circ_{37})/310.15$.

between G and U in G·U mismatches in the various oligomers are sequence dependent. The NOE data are summarized in Table IV, and the assignments are indicated in Figure 2. The imino proton resonances for the G·U mismatches are between 10.8 and 12.0 ppm. This is consistent with the shifts of 10.43 and 11.78 ppm observed for a G·U mismatch in tRNA (Johnston & Redfield, 1981).

Imino proton spectra of GGAGUUCC and GGAUGUCC at different temperatures are shown in Figure 4. For GGAGUUCC, the G·U imino proton resonances broaden before those of the internal Watson–Crick base pairs in the same molecule. Similar results are observed for GUCGUGAC and CCUGUAGG (data not shown). In contrast, for

Table IV: Summary of NOE Data[a]

oligomers	irradiated resonances: position[b] (ppm)	line width[c] (Hz)	assignments[d]	NOEs: position[b] (ppm)	assignments[d]	fractional transfer[e]
1 2 3 4 5 6 7 8 5′GGAGUUCC3′ 3′CCUUGAGG5′ 8 7 6 5 4 3 2 1	14.3	27	U6	7.5	A3 H2	0.15
	14.3			11.7	G4 or U5	0.1
	14.3			12.0	G4 or U5	0.07
	14.3			12.5	G2	0.15
	12.5	37	G2	14.3	U6	w
	12.0	28	G4 or U5	11.7	G4 or U5	0.34
	11.7	33	G4 or U5	12.0	G4 or U5	0.44
1 2 3 4 5 6 7 8 5′GGAUGUCC3′ 3′CCUGUAGG5′ 8 7 6 5 4 3 2 1	14.4	20	U6	7.9	A3 H2	0.18
	14.4			11.2	U4 or G5	0.16
	14.4			11.8	U4 or G5	0.16
	14.4			12.5	G2	0.08
	12.5	33	G2	11.2	U4 or G5	w
	12.5			11.8	U4 or G5	w
	12.5			14.4	U6	w
	11.8	22	U4 or G5	11.2	U4 or G5	0.25
	11.8			12.5	G2	w
	11.8			14.4	U6	0.07
	11.2	23	U4 or G5	11.8	U4 or G5	0.29
	11.2			12.5	G2	w
	11.2			14.4	U6	0.09
1 2 3 4 5 6 7 8 5′CCUGUAGG3′ 3′GGAUGUCC5′ 8 7 6 5 4 3 2 1	14.4	19	U3	7.8	A6 H2	0.17
	14.4			11.2	G4 or U5	0.07
	14.4			11.8	G4 or U5	0.12
	14.4			12.5	G7	0.07
	12.5	18	G7	11.8	G4 or U5	0.08
	11.8	20	G4 or U5	11.2	G4 or U5	0.22
	11.8			14.4	U6	0.05
	11.2	17	G4 or U5	11.8	G4 or U5	0.38
	11.2			14.4	U6	0.06
1 2 3 4 5 6 7 8 5′GUCGUGAC3′ 3′CAGUGCUG5′ 8 7 6 5 4 3 2 1	14.8	36	U2	7.8	A7 H2	0.21
	14.8			12.2	G6	0.14
	14.8			13.0	G1	0.07
	13.0	88	G1	14.8	U2	0.09
	12.2	38	G6	14.8	U2	0.04
	11.8	42	G4 or U5	10.9	G4 or U5	0.16
	11.8			12.2	G6	w
	10.9	51	G4 or U5	11.8	G4 or U5	0.17
	10.9			12.2	G6	w

[a] Spectra were taken at 0.5 °C for GUCGUGAC, CCUGUAGG, and GGAGUUCC and at 5 °C for GGAUGUCC. Other conditions are the same as in Figure 2. One-second saturation was used and saturation power levels were adjusted to result in about 80% saturation of the desired resonance. [b] Peak positions are referenced to TSP. [c] Full width at half-maximum height with 4 Hz line broadening. [d] Discussed in the text. [e] Integrated area of NOE peak divided by integrated area of saturated peak. w means fractional transfer is less than 0.04.

GGAUGUCC, the G·U imino protons are as sharp as other internal base pairs at high temperature.

Imino proton spectra for the non-two-state molecules GGUGUACC, UGGCUA, and GUAGCUGC are shown in Figure 5. There are two more peaks than expected in the spectra of GGUGUACC and UGGCUA, suggesting slow chemical exchange. Furthermore, the relative intensities of the resonances between 13.0 and 14.5 ppm change with temperature (spectra not shown), indicating a change in the populations of the exchanging structures. For GUAGCUGC, there are five imino proton resonances as expected. When temperature is increased, no new peaks appear. At 20 °C, the resonance at ca. 11.7 ppm disappears, the resonance at ca. 13.1 ppm becomes broad, and the other three peaks do not change much (spectra not shown). This is unusual because the resonances at 11.7 and 11.0 ppm likely arise from the G·U pair. For all other sequences containing G·U mismatches, the two G·U resonances broaden and disappear together.

Discussion

The most surprising results from this work concern the nearest neighbor $^{5'GU3'}_{3'UG5'}$. Addition of $^{5'GU3'}_{3'UG5'}$ to the middle of a helix in the contexts $^{CGUG}_{GUGC}$, $^{UGUA}_{AUGU}$, and $^{AGUU}_{UUGA}$ destabilizes the helix. A nearest-neighbor analysis containing $^{5'GU3'}_{3'UG5'}$ in only these contexts gives an unfavorable $\Delta G°_{37}$ of +1.5 kcal/mol for the $^{5'GU3'}_{3'UG5'}$ interaction. Addition of $^{5'GU3'}_{3'UG5'}$ to the middle of a helix in the context $^{GGUC}_{CUGG}$, however, stabilizes the helix. A nearest-neighbor analysis containing $^{5'GU3'}_{3'UG5'}$ in only this context gives a favorable $\Delta G°_{37}$ of −1.0 kcal/mol for the $^{5'GU3'}_{3'UG5'}$ interaction. This is a non-nearest-neighbor effect. In contrast, the nearest neighbor $^{5'UG3'}_{3'GU5'}$ is always stabilizing, and the nearest-neighbor $\Delta G°_{37}$ for $^{5'UG3'}_{3'GU5'}$ is apparently independent of context. The unfavorable $\Delta G°_{37}$ for $^{5'GU3'}_{3'UG5'}$ in certain contexts is grossly different from the favorable −0.5 kcal/mol currently assigned to this nearest neighbor for prediction of RNA secondary structure (Freier et al., 1986a; Turner et al., 1988). The previous parameter was estimated since no oligomers with a $^{5'GU3'}_{3'UG5'}$ motif had been studied. In the secondary structures for a set of 16S (Gutell et al., 1985) and 23S (Gutell et al., 1988) rRNAs, there are 98 $^{5'UG3'}_{3'GU5'}$ but only 10 $^{5'GU3'}_{3'UG5'}$ nearest neighbors. This suggests that the phylogenetic preference for UG over GU may have a thermodynamic basis. It also suggests the parameters measured for these nearest neighbors may improve predictions of secondary structure.

CD and imino proton NMR studies of the sequences GUCGUGAC, CCUGUAGG, GGAGUUCC, and GGAU-

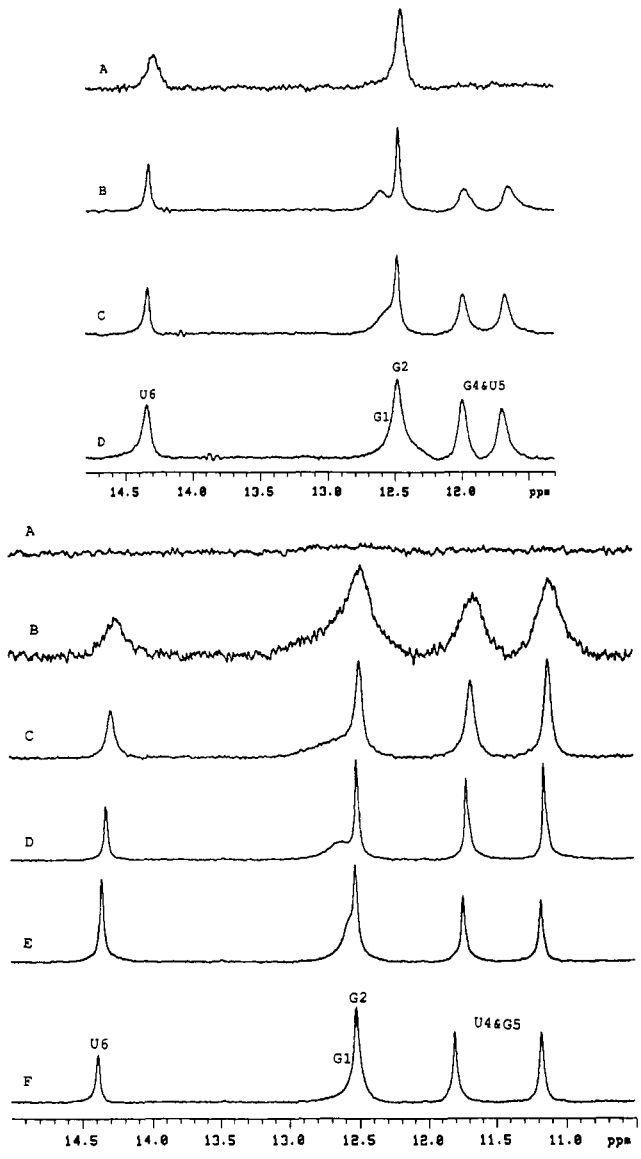

FIGURE 4: (Top) Imino proton spectra (500 MHz) of GGAGUUCC at 30 °C (A), 15 °C (B), 10 °C (C), and 0.5 °C (D). Other conditions are the same as in Figure 2. Assignments are shown above spectrum D. (Bottom) Imino proton spectra (500 MHz) of GGAUGUCC at 50 °C (A), 45 °C (B), 40 °C (C), 30 °C (D), 20 °C (E), and 10 °C (F). Other conditions are the same as in Figure 2. Assignments are shown above spectrum F.

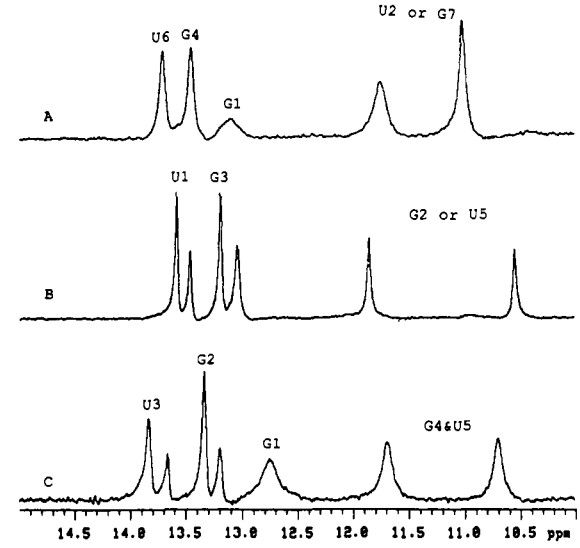

FIGURE 5: Imino proton spectra (500 MHz) of GUAGCUGC at 1 °C (A), UGGCUA at 1 °C (B), and GGUGUACC at 20 °C (C). Other conditions are the same as in Figure 2. Preliminary assignments are shown above each spectrum.

GUCC do not reveal any obvious reason for the difference between $\frac{5'GU3'}{3'UG5'}$ and $\frac{5'UG3'}{3'GU5'}$ nearest neighbors. There is no large difference in the CD spectra from 240 to 300 nm, as might be observed for a major change in helix conformation (Tunis-Schneider & Maestre, 1970; Hall et al., 1984). All four sequences exhibit resonances for five imino protons, including two from each G·U mismatch (Figure 2). The strengths of the NOEs between the imino protons in the G·U mismatches can be compared with those between imino protons of adjacent Watson–Crick base pairs and between the imino proton in the A·U base pair and the adenine H2 in each duplex (see Table IV). Except for GUCGUGAC, the NOEs between the imino protons in the G·U mismatches are stronger than both the NOE between internal adjacent G·C and A·U pairs and the NOE between the imino proton in the A·U base pair and the A H2 in the same helix. This suggests the distance between the imino protons in the G·U mismatches is about 3 Å, consistent with wobble-type hydrogen bonding as suggested by Crick (1966). While the hydrogen-bonding pattern appears similar in CCUGUAGG, GGAGUUCC, and GGAUGUCC, the thermodynamics are different. Insertion of the GU sequence makes the free energy of duplex formation less favorable by 1 kcal/mol, whereas insertion of the UG sequence makes it more favorable by 1 kcal/mol (see Table II). Thus the number of hydrogen bonds formed is not the only factor determining stability.

For GUCGUGAC, the NOEs between the imino protons in the G·U mismatches are about the same as the NOE between the U2 and G6 imino protons and weaker than the NOE between the imino proton in the A·U base pair and the A H2. This may be due to an imino–imino proton distance longer than 3 Å and/or chemical exchange for the imino protons. The line widths of all the imino resonances for GUCGUGAC are broader than those for the other sequences (see Figure 2), consistent with chemical exchange.

While most adjacent G·U mismatches have the same hydrogen-bonding pattern, the temperature dependence of the resonances is different for UG and GU sequences. When temperature is raised, the imino resonances for G·U mismatches and Watson–Crick base pairs in GGAUGUCC broaden at the same temperature. In contrast, for GGAGUUCC, GUCGUGAC, and CCUGUAGG, the resonances for the G·U mismatches broaden at much lower temperatures than the resonances for the Watson–Crick base pairs in the same duplex. This suggests the hydrogen bonding and/or stacking in G·U mismatches is weaker for $\frac{5'GU3'}{3'UG5'}$ than for $\frac{5'UG3'}{3'GU5'}$ sequences. This is consistent with the relative thermodynamic stabilities.

The structural conclusions from the spectroscopic studies can be compared with results from X-ray diffraction studies of the deoxyoligonucleotides d(GGGTGCCC) and d(GGGGTCCC) (Kneale et al., 1985; Rabinovich et al., 1988). These sequences crystallize as A-form duplexes, the geometry expected for RNA duplexes. The helical parameters are similar to those for the fully matched duplex, d(GGGCGCCC) (Rabinovich et al., 1988), suggesting G·T mismatches can be accommodated in A-form geometry. All the G·T mismatches have two hydrogen bonds involving imino protons. Stacking patterns for the GT and TG sequences are different, however.

Thus the results for the RNA sequences studied here are consistent with expectations from the crystal structures of the DNA sequences.

When sequences containing $\overset{GGUC}{CUGG}$ and/or $\overset{CGUG}{GUGC}$, $\overset{UGUA}{AUGU}$, and $\overset{AGUU}{UUGA}$ are omitted, thermodynamic parameters for all the remaining apparently two-state sequences in Table II are fit well with a nearest-neighbor analysis. This indicates that within the limits of the model and experimental error, terminal and internal G·U mismatches have the same nearest-neighbor stability increments. Current algorithms for prediction of RNA secondary structure also assume equivalence of terminal and internal G·Us (Turner et al., 1988; Jaeger et al., 1989).

Table III contains experimentally determined nearest-neighbor parameters for all 11 possible combinations of G·U mismatches with Watson–Crick pairs or another G·U mismatch. The number of duplexes containing each nearest-neighbor ranges from one to six with an average of three. Thus it is likely these parameters can be improved by further studies. Nevertheless, it is interesting to compare these results with nearest-neighbor parameters for Watson–Crick pairs (Freier et al., 1986a). On average, a G·U mismatch adjacent to a Watson–Crick pair is only 0.2 kcal/mol less stable than the corresponding AU base pair. For nearest neighbors involving at least one Watson–Crick pair, the most stable sequences have a 5′ G. This includes five of the six most stable nearest neighbors with G·U mismatches (see Table III) and the four most stable with two Watson–Crick pairs (Freier et al., 1986a). The results suggest a 5′ G allows a particularly favorable interaction in RNA.

The non-nearest-neighbor effects and the nearest-neighbor parameter for $\overset{5'GU3'}{3'UG5'}$ are surprising. The non-two-state melting and unusual NMR characteristics for GGUGUACC, UGGCUA, and GUAGCUGC are also surprising. Evidently, not enough is known about interactions determining RNA stability to permit reliable predictions for new motifs. In principle, such predictions could be made with free energy perturbation and other methods based on quantum mechanics (McCammon & Harvey, 1987; Bash et al., 1987). The results presented here should provide good tests for such methods. Some of the sequences should also provide good model systems for detailed structural studies aimed at uncovering the interactions determining stability.

Supplementary Material Available

One figure with CD spectra and one table with thermodynamic parameters and errors for all duplexes used in nearest-neighbor analysis (4 pages). Ordering information is given on any current masthead page.

References

Albergo, D. D., Marky, L. A., Breslauer, K. J., & Turner, D. H. (1981) *Biochemistry 20*, 1409–1413.

Alkema, D., Hader, P. A., Bell, R. A., & Neilson, T. (1982) *Biochemistry 21*, 2109–2117.

Bash, P. A., Singh, U. C., Langridge, R., & Kollman, P. A. (1987) *Science 236*, 564–568.

Bevington, P. R. (1969) *Data Reduction and Error Analysis for the Physical Sciences*, McGraw-Hill, New York.

Borer, P. N., Dengler, B., Tinoco, I., Jr., & Uhlenbeck, O. C. (1974) *J. Mol. Biol. 86*, 843–853.

Breslauer, K. J., Sturtevant, J. M., & Tinoco, I., Jr. (1975) *J. Mol. Biol. 99*, 549–565.

Burke, J. M., Belfort, M., Cech, T. R., Davies, R. W., Schweyen, R. J., Shub, A., Szostak, J. W., & Tabak, J. F. (1987) *Nucleic Acids Res. 18*, 7217–7221.

Cantor, C. R., & Schimmel, P. R. (1980) *Biophysical Chemistry Part II*, Chapter 8, W. H. Freeman, San Francisco, CA.

Cech, T. R., Tanner, N. K., Tinoco, I., Jr., Weir, B. R., Zuker, M., & Perlman, P. S. (1983) *Proc. Natl. Acad. Sci. U.S.A. 80*, 3903–3907.

Chou, S.-H., Flynn, P., & Reid, B. (1989) *Biochemistry 28*, 2422–2435.

Crick, F. H. C. (1966) *J. Mol. Biol. 19*, 548–555.

Davies, R. W., Waring, R. B., Ray, R. A., Brown, T. A., & Scazzocchio, C. (1982) *Nature 300*, 719–724.

Erdmann, V. A., Wolters, J., Huysmans, E., & DeWachter, R. (1985) *Nucleic Acids Res. 13*, r105–r153.

Fox, G. E., & Woese, C. R. (1975) *Nature (London) 256*, 505–506.

Freier, S. M., Burger, B. J., Alkema, D., Neilson, T., & Turner, D. H. (1983) *Biochemistry 22*, 6198–6202.

Freier, S. M., Kierzek, R., Jaeger, J. A., Sugimoto, N., Caruthers, M. H., Neilson, T., & Turner, D. H. (1986a) *Proc. Natl. Acad. Sci. U.S.A. 83*, 9373–9377.

Freier, S. M., Kierzek, R., Caruthers, M. H., Neilson, T., & Turner, D. H. (1986b) *Biochemistry 25*, 3209–3213.

Gutell, R. R., & Fox, G. E. (1988) *Nucleic Acids Res. 16* (Suppl.), r175–r269.

Gutell, R. R., Weiser, B., Woese, C. R., & Noller, H. F. (1985) *Prog. Nucleic Acids Res. Mol. Biol. 32*, 155–216.

Hall, K., Cruz, P., Tinoco, I., Jr., Jovin, T. M., & van de Sande, J. H. (1984) *Nature 311*, 584–586.

Hickey, D. R., & Turner, D. H. (1985) *Biochemistry 24*, 2086–2094.

Hore, P. J. (1983) *J. Magn. Reson. 55*, 283–300.

Jaeger, J. A., Turner, D. H., & Zuker, M. (1989) *Proc. Natl. Acad. Sci. U.S.A. 86*, 7706–7710.

Johnston, P. D., & Redfield, A. D. (1981) *Biochemistry 20*, 1147–1156.

Kierzek, R., Caruthers, M. H., Longfellow, C. E., Swinton, D., Turner, D. H., & Freier, S. M. (1986) *Biochemistry 25*, 7840–7846.

Kim, S.-H., & Cech, T. R. (1984) *Proc. Natl. Acad. Sci. U.S.A. 84*, 8788–8792.

Kim, S.-H., Suddath, F. L., Quigley, G. J., McPherson, A., Sussman, J. L., Wang, A. H. J., Seeman, N. C., & Rich, A. (1974) *Science (Washington, D.C.) 185*, 435–440.

Kime, M. J., & Moore, P. B. (1983) *Biochemistry 22*, 2615–2622.

Kneale, G., Brown, T., Kennard, O., & Rabinovich, D. (1985) *J. Mol. Biol. 186*, 805–814.

Ladner, J. E., Jack, A., Robertus, J. D., Brown, J. W., Rhodes, D., Clarke, B. F. C., & Klug, A. (1975) *Proc. Natl. Acad. Sci. U.S.A. 72*, 4414–4418.

Markiewicz, W. T., Biala, E., & Kierzek, R. (1984) *Bull. Pol. Acad. Sci. Chem. 32*, 433–451.

McCammon, J. A., & Harvey, S. C. (1987) *Dynamics of Proteins and Nucleic Acids*, Cambridge University Press, Cambridge, England.

Michel, F., & Westhof, E. (1990) *J. Mol. Biol. 216*, 585–610.

Michel, F., Jacquier, A., & Dujon, B. (1982) *Biochimie 64*, 867–861.

Milligan, J. F., Groebe, D. R., Witherell, G. W., & Uhlenbeck, O. C. (1987) *Nucleic Acids Res. 15*, 8783–8798.

Noller, H. F. (1984) *Annu. Rev. Biochem. 53*, 119–162.

Petersheim, M., & Turner, D. H. (1983) *Biochemistry 22*, 256–263.

Rabinovich, D., Haran, T., Eisenstein, M., & Shakked, Z. (1988) *J. Mol. Biol. 200*, 151–161.
Romaniuk, P. J., Hughes, D. W., Gregoire, R. J., Bell, R. A., & Neilson, T. (1979a) *Biochemistry 18*, 5109–5116.
Romaniuk, P. J., Hughes, D. W., Gregoire, R. J., Neilson, T., & Bell, R. A. (1979b) *J. Chem. Soc., Chem. Commun.*, 559–560.
SantaLucia, J., Jr., Kierzek, R., & Turner, D. H. (1991a) *J. Am. Chem. Soc. 113*, 4313–4322.
SantaLucia, J., Jr., Kierzek, R., & Turner, D. H. (1991b) *Biochemistry 30*, 8242–8251.
Sprinzl, M., Moll, J., Meissner, F., & Hartman, T. (1985) *Nucleic Acids Res. 13*, r1–r49.
Steger, G., Hofmann, H., Fortsch, J., Gross, H. J., Randles, J. W., Sanger, H. L., & Riesner, D. (1984) *J. Biomol. Struct. Dyn. 2*, 543–571.
Stern, S., Weiser, B., & Noller, H. F. (1988) *J. Mol. Biol. 204*, 447–481.
Sugimoto, N., Kierzek, R., Freier, S. M., & Turner, D. H. (1986) *Biochemistry 25*, 5755–5759.
Sugimoto, N., Kierzek, R., & Turner, D. H. (1987) *Biochemistry 26*, 4559–4562.
Sussman, J. L., & Kim, S. H. (1976) *Biochem. Biophys. Res. Commun. 68*, 89–96.
Tinoco, I., Jr., Uhlenbeck, O. C., & Levine, M. (1971) *Nature 230*, 362–367.
Tinoco, I., Jr., Borer, P. N., Dengler, B., Levine, M. D., Uhlenbech, O. C., Crothers, D. M., & Gralla, J. (1973) *Nature (London) New Biol. 246*, 40–41.
Tunis-Schneider, M. J. B., & Maestre, M. F. (1970) *J. Mol. Biol. 52*, 521–541.
Turner, D. H., Sugimoto, N., & Freier, S. M. (1988) *Annu. Rev. Biophys. Biophys. Chem. 17*, 167–192.
Uhlenbeck, O. C., Martin, F. H., & Doty, P. (1971) *J. Mol. Biol. 57*, 217–229.
Usman, N., Ogilvie, K. K., Jiang, M. Y., & Cedergren, R. L. (1987) *J. Am. Chem. Soc. 109*, 7845–7854.
Watson, J. D., Hopkins, N. H., Roberts, J. W., Steitz, J. A., & Weiner, A. M. (1987) *Molecular Biology of the Gene*, Benjamin Cummings, Inc., Menlo Park, CA.
Wentworth, W. E. (1965) *J. Chem. Educ. 42*, 96–167.
Woese, C. R., Gutell, R., Gupta, R., & Noller, H. F. (1983) *Microbiol. Rev. 47*, 621–669.
Zuker, M. (1989) *Science 244*, 48–52.